Mean Aneurysm Flow Amplitude Ratio Comparison between DSA and CFD

Fred van Nijnatten[1,*], Odile Bonnefous[2,*], Hernan G. Morales[2], Thijs Grünhagen[1], Roel Hermans[1], Olivier Brina[3], Vitor Mendes Pereira[3,4], Daniel Ruijters[1]

[1] interventional X-Ray, Philips Healthcare, Best, The Netherlands
{fred.van.nijnatten,thijs.grunhagen,roel.hermans,
danny.ruijters}@philips.com
[2] Medisys - Philips Research, Paris, France
{odile.bonnefous,hernan.morales}@philips.com
[3] Division of Neuroradiology, Department of Medical Imaging,
University Hospitals of Geneva, Switzerland
olivier.brina@hcuge.ch
[4] Division of Neuroradiology, Department of Medical Imaging and Division of Neurosurgery,
Department of Surgery, Toronto Western Hospital,
University Health Network, Toronto, Ontario, Canada
vitormpbr@hotmail.com

Abstract. The Mean Aneurysm Flow Amplitude ratio (MAFA-ratio) has been proposed to evaluate the efficacy of flow diverting stents during minimally invasive intracranial aneurysm treatment. A method has been described for calculating the MAFA-ratio on high frame-rate digital subtraction angiography (DSA) acquisitions using an optical flow algorithm. In this article we have generated computational fluid dynamics (CFD) simulations using six distinct aneurysms and computed the MAFA-ratios based on these data. Furthermore, the simulations have been used to create virtual angiograms, in order to calculate the MAFA-ratios using the DSA approach. An analysis of the MAFA-ratios generated by both methods shows that there is a monotone increasing relation between the DSA and CFD based ratios, albeit without a slope being identity. Overall, it can be concluded that the DSA-based ratio is a predictor for the magnitude of aneurysm flow reduction, i.e., for the efficacy of flow diverting stents.

Keywords: Mean aneurysm flow amplitude, Flow diversion, Digital subtraction angiography, Computational fluid dynamics.

1 Introduction

Digital subtraction angiography (DSA) and three-dimensional rotational angiography (3DRA) are currently the gold standard for imaging and navigation of intravascular

[*] Fred van Nijnatten and Odile Bonnefous are joint first authors.

N. Navab et al. (Eds.): MICCAI 2015, Part II, LNCS 9350, pp. 485–492, 2015.
DOI: 10.1007/978-3-319-24571-3_58

devices during minimally invasive intracranial aneurysm treatment. While traditional DSA and 3DRA are unrivalled regarding imaging the vascular morphology, they lack functional information. Recently, aneurysm treatment by flow diverting stents has been gaining popularity. These devices reduce the inflow of blood into the aneurysm with the objective to cause the blood in the aneurysm to thrombose in the months following the intervention. The reduction of blood inflow causes flow alterations in both amplitude and patterns in the aneurysm sac, which are considered to predict rupture and clotting [1,2,3,4].

A linear dependency between the amplitude of the aneurysm flow and the arterial flow rate in the feeding vessel has been shown in [5]. Therefore, the possible variation of arterial flow conditions should be taken into account when evaluating the aneurysm flow reduction induced by a flow diverter. This can be achieved by normalization of aneurysm flow measurements with their corresponding arterial flow measurements.

The normalized mean aneurysm flow amplitude ratio (MAFA-ratio) has been introduced as a parameter that can be used to measure the efficacy of the flow diverting stent during the course of the intervention [6,7,8]. The MAFA-ratio R is defined as:

$$R = \frac{M_{post}}{M_{pre}} \cdot \frac{Q_{pre}}{Q_{post}} \tag{1}$$

Whereby the *pre* and *post* subscripts indicate measured quantities prior and after deploying the flow diverting stent. Q represents the time-averaged arterial flow of the feeding parent blood vessel, which is used to normalize the MAFA-ratio for overall flow changes [9]. The mean flow in the aneurysm sac M is calculated as follows:

$$M = \frac{\int_T \int_V \left|\vec{v}(\vec{x},t)\right| d\vec{x}dt}{\int_T \int_V d\vec{x}dt} \tag{2}$$

Whereby T is the time window, t represents time, V the aneurysm sac volume, $\vec{x}$ position, and $\vec{v}$ blood velocity.

The MAFA-ratio can be measured peri-interventionally using high frame-rate DSA sequences. During the acquisition of the DSA data, iodine contrast agent is injected intra-arterially at a very modest pace (1.5 ml/s). The contrast agent is consequently modulated by the flow pulsatility at the injection point, driven by the cardiac cycle. The contrast will be denser during the diastole phase and less dense during the systole phase. The modulated contrast agent pattern travels through the vessels and aneurysm sac, and is followed using an optical flow algorithm [10].

2 Methods

In this article, we compare the MAFA-ratios calculated from computational fluid dynamics (CFD) with high frame-rate DSA (60 fps) calculations. For this purpose, CFD simulations were performed, using 3DRA reconstructions of intracranial aneurysms acquired from six patients, see Figure 1. All aneurysms were located on the internal carotid artery. Aneurysm size ranged from small (5mm) to large (15mm), see Table 1.

Nine CFD input flow conditions were imposed for each 3DRA, with mean flow rates ranging from 1 ml/s to 5 ml/s in increments of 0.5 ml/s. The arterial flow curves were created by scaling a reference flow curve as described in [5,9]. Hexahedral meshes were generated from the vasculature segmented in the 3DRA data with the SnappyHexMesh utility from OpenFoam. The CFD simulations were performed with OpenFoam v2.2.1.

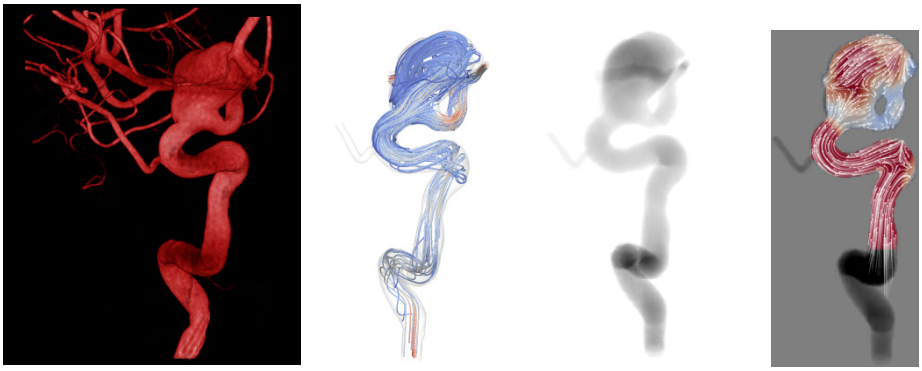

(a) (b) (c) (d)

Fig. 1. (a) 3DRA reconstruction of an intracranial aneurysm. (b) Computational fluid simulation (CFD), whereby the stream lines illustrate the 3D vector field. (c) Virtual angiogram view generated from the CFD data. (d) 2D flow field obtained by the optical flow algorithm from the contrast motion in the time dependent virtual angiograms.

Table 1. Aneurysm dimensions.

Patient nr.	1	2	3	4	5	6
Largest diameter (mm)	8.3	15.0	5.3	5.1	8.0	7.6

The CFD simulations were performed without and with virtual stents placed, as described in [5,9]. The first stent had a porosity of 0.72, which is chosen to mimic the Silk flow diverter stent. Two additional CFD simulations were performed for three out of six aneurysms. One with a stent having a porosity of 0.92, and another one also with a porosity of 0.92, but this time the stent did not fully cover the aneurysm ostium to mimic an ill-positioned stent. The CFD simulations yielded a time-dependent 3D vector field representing the displacements of blood, which was used to calculate the space and time averaged CFD aneurysm flow.

The CFD simulations were also used to generate virtual angiograms from two different viewing angles [3], see Fig. 1. The virtual angiograms were loaded in the Aneurysm Flow software (Philips Healthcare, Best, the Netherlands) to compute the mean aneurysm flow and arterial flow based on high frame-rate DSA. The mean flow for the CFD data was calculated on the 3D flow vector field, whereas the flow for the DSA data was computed on the 2D projection images, using an optical flow algorithm [10].

The simulations allowed to perform a lot of experiments while varying selected parameters while keeping others the same, which would not have been possible in-vivo. The following conditions were varied in the experiments:

- Six 3DRA geometries of different aneurysms.
- Nine flow rates: ranging from 1 ml/s to 5 ml/s in increments of 0.5 ml/s.
- CFD simulations: without stent, with stent 1 with porosity 0.72, with stent 2 with porosity 0.92 (for three aneurysms), with ill-positioned stent 3 with porosity 0.92 (for three aneurysms).
- Two projection angles for the virtual angiograms.

In total 9*4=36 CFD simulations were performed for the first three aneurysms and 9*2=18 simulations for the second three aneurysms, yielding a total of 36+18=54 CFD simulations. Per simulation two virtual angiograms were computed from different projection angles, delivering in total 108 virtual angiograms.

MAFA-ratios were computed from two angiograms for the same aneurysm and the same projection angle, one without stent and one with stent, whereby the difference in pre- and post-deployment arterial flow was ≤ 1.5 ml/s. This range was selected based on the analysis of arterial flow changes prior and after stenting in 61 clinical cases. This yielded 9+8+8+7+7+6+6=51 ratios for each aneurysm-stent-view combination.

3 Results

The MAFA-ratio computed on the virtual angiograms is plotted versus the MAFA-ratio computed on the CFD data for each aneurysm. Figure 2 presents an example of such a graph. From this data, available for every aneurysm, the average and standard deviation of the MAFA-ratios are calculated for each aneurysm-stent combination, see Fig. 3. A regression line fitted through these points delivers: $y = 0.68 \cdot x + 0.34$, with the coefficient of determination r^2 being 0.96.

Furthermore, the pooled standard deviation σ_p is computed from the standard deviations that are calculated for each aneurysm-stent combination as follows:

$$\sigma_p = \sqrt{\frac{\sum (n_i - 1) \cdot \sigma_i^{\,2}}{\sum (n_i - 1)}} \tag{3}$$

Whereby n_i is the size of a stent group of aneurysm i and σ_i the standard deviation of a stent group of aneurysm i. The average MAFA-ratios for the stents are presented in Table 2, while the results of the pooled standard are provided in Table 3.

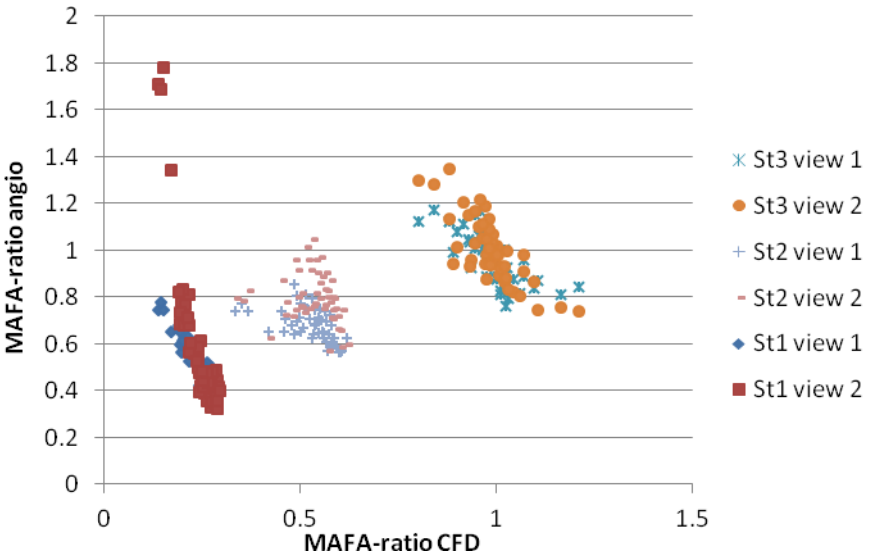

Fig. 2. For a particular aneurysm geometry (patient 2) the MAFA-ratio based on the virtual angiograms (vertical axis) is plotted versus the MAFA-ratio based on the CFD vector fields (horizontal axis). The MAFA-ratio was calculated for three simulated stents; stent 1 (St1) has a porosity of 0.72, stent 2 (St2) a porosity of 0.92 and stent 3 (St3) also a porosity of 0.92, but is ill-deployed. Each view number represents a distinct projection angle.

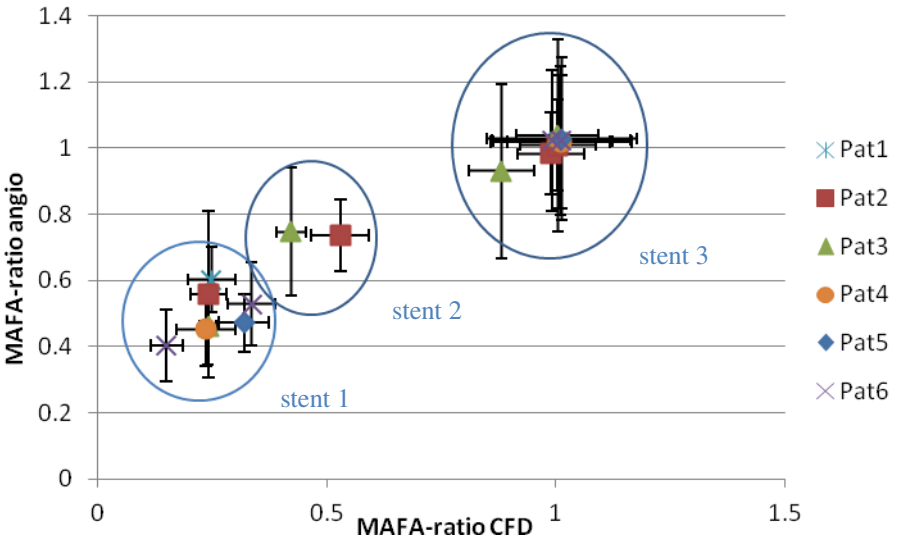

Fig. 3. Average MAFA-ratio based on the virtual angiograms (vertical axis) vs. average MAFA-ratio based on CFD (horizontal axis) for each aneurysm-stent combination. The averages are computed over both views combined. The error bars indicate the standard deviation.

Finally, the pooled standard deviation for the two combined DSA views is evaluated as a function of the absolute arterial flow difference $\Delta Q = |Q_{post} - Q_{pre}|$, as shown in Fig. 4.

Table 2. Average MAFA-ratio for the three different stents and without stent.

Average	CFD	View 1	View 2	View 1&2
Stent 1	0.24	0.49	0.50	0.49
Stent 2	0.43	0.70	0.64	0.67
Stent 3	0.95	0.98	0.98	0.98
Without stent	1.01	1.02	1.02	1.02

Table 3. Pooled standard deviation of the three different stents and without stent.

Pooled stddev. σ_p	CFD	View 1	View 2	View 1&2
Stent 1	0.05	0.11	0.16	0.14
Stent 2	0.05	0.15	0.11	0.15
Stent 3	0.09	0.21	0.21	0.21
Without stent	0.13	0.23	0.22	0.22

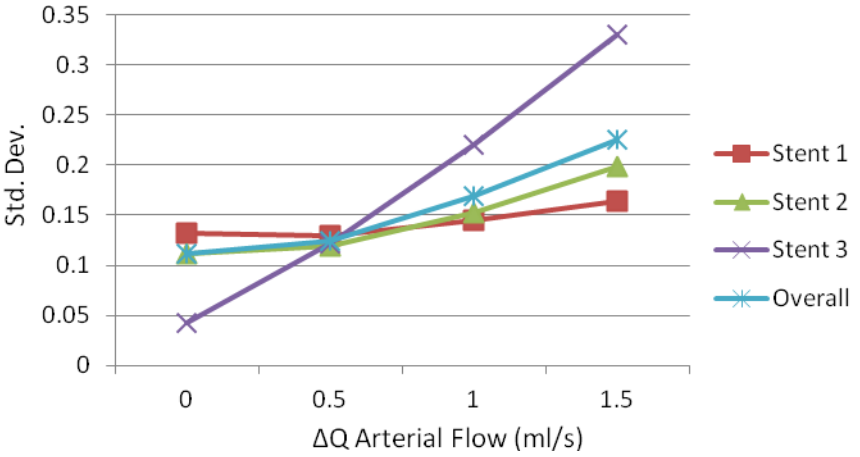

Fig. 4. Pooled standard deviation (vertical axis) from the combined views 1 & 2 for each stent, and overall (combined data of view 1 and 2) for all stents together, as a function of the ΔQ absolute arterial flow difference (horizontal axis).

4 Discussion

In the ideal case, the six stent-view combinations would show up as three points in Fig. 2 without any spread. This would mean that there is no difference in the MAFA-ratio if you would choose a different viewing angle, and that the MAFA-ratio is invariant to

changes in arterial flow. Each stent, however, yields a distinct cloud of points in the plot that compares the MAFA-ratios computed from the virtual angiograms and from the CFD data, as can be seen in Fig. 2. The point clouds produced by the two different projection angles map very well on each other. This trend is also observed for the other five aneurysms.

The data for all aneurysms are represented in a single graph (Fig. 3), whereby each data point represents the mean and standard deviation for each aneurysm-stent combination. The data points appear to represent a linear relation nearly passing through coordinate (1,1), which indicates that when the CFD MAFA-ratio indicates no flow reduction (R=1), the DSA MAFA-ratio indicates the same (R=1), independently of the projection angle. For the stents we expect lower MAFA-ratios for lower porosity values, as can be observed in Table 2 and Fig. 3. A flow reduction ($R < 1$) also is confirmed in both measurements, and a stronger reduction ($R_1 < R_2$) is also consistently found in both CFD and DSA measurements, due to their monotone increasing relation.

In the ideal case, the MAFA-ratios of the angiograms would be exactly equal to the MAFA-ratios of the CFD. However, the slope of the relation is not 1, which might be caused by the differences between the dimensionality of the two methods; The CFD MAFA-ratio is calculated in 3D space, whereas the DSA MAFA-ratio is obtained in a projective 2D space, which suffers from phenomena like foreshortening, overlapping structures, laminar flow effects, etc. This means that threshold analysis performed on one technique (e.g., CFD) cannot be applied to the other one (e.g., DSA).

The standard deviation of the aneurysm-stent combinations is presented in Fig. 3 as horizontal bars for the CFD and vertical bars for the DSA. While the averages of the various stents for a clear trend, there is overlap of the standard deviations on the vertical axis, which has implications on the predictive power of a single DSA-based MAFA measurement, and should be taken into account when determining safety margins around clinically relevant thresholds.

The fact that also the CFD simulations possess a standard deviation > 0 implies that the normalization by the arterial flow in Equation 1 is not perfect. This is confirmed in Figure 4, where a larger difference between pre- and post-deployment arterial flow tends to increase the standard deviation. This effect is stronger when the MAFA-ratio R is close to 1, as is the case with stent 3 (see also Table 3). This phenomenon might be caused by phenomena like the development of vortices and unsteady flow features, and by a non-linear relation between the aneurysm flow magnitude and the arterial flow, due to the ratio of shear flow versus influx flow being dependent on the arterial flow magnitude. Furthermore, the normalized MAFA-ratio definition does not take any bias effects into account [5], which may have an impact on the standard deviation. Future research might investigate this effect further. In clinical practice this can be taken into account by applying a larger safety margin to a chosen threshold when the arterial flow differs more.

5 Conclusion

In this article we have examined the relation between the MAFA-ratios obtained directly from CFD simulations with the DSA based MAFA-ratios by generating virtual angiograms from the CFD data. We have found that while the slope of a regression line

through the ratios is not 1, the ratios have a monotone increasing relation and correspond in predicting (practically) no flow reduction, as well as increasingly stronger reductions. Therefore, it can be concluded that the DSA-based MAFA-ratio can be used as a tool in interventional intracranial aneurysm treatment to evaluate the efficacy of a flow diverting stent. Since the slope of the DSA-based MAFA-ratios and the CFD-based ratios is not the identity, any threshold analysis to associate a MAFA-ratio range with certain clinical outcome is only valid for the respective technique used to acquire the input data of that analysis.

References

1. Augsburger, L., Reymond, P., Fonck, E., Kulcsar, Z., Farhat, M., Ohta, M., Stergiopulos, N., Rüfenacht, D.A.: Methodologies to assess blood flow in cerebral aneurysms: Current state of research and perspectives. J. Neuroradiol. 36, 270–277 (2009)
2. Sforza, D.M., Putman, C.M., Cebral, J.R.: Hemodynamics of cerebral aneurysms. Annu. Rev. Fluid Mech. 41, 91–107 (2009)
3. Sun, Q., Groth, A., Bertram, M., Waechter, I., Bruijns, T., Hermans, R., Aach, T.: Phantom-based experimental validation of computational fluid dynamics simulations on cerebral aneurysms. Med. Phys. 37, 5054–5065 (2010)
4. Groth, A., Waechter-Stehle, I., Brina, O., Perren, F., Mendes Pereira, V., Rüfenacht, D., Bruijns, T., Bertram, M., Weese, J.: Clinical study of model-based blood flow quantification on cerebrovascular data. In: Wong, K.H., Holmes III, D.R. (eds.) SPIE Medical Imaging: Visualization, Image-Guided Procedures, and Modeling, vol. 7964, pp. 79640X. SPIE Press (2011)
5. Morales, H.G., Bonnefous, O.: Unraveling the relationship between arterial flow and intra-aneurysmal hemodynamics. J. Biomech. 48, 585–591 (2015)
6. Mendes Pereira, V., Bonnefous, O., Ouared, R., Brina, O., Stawiaski, J., Aerts, H., Ruijters, D., Narata, A.P., Bijlenga, P., Schaller, K., Lovblad, K.-O.: A DSA-Based Method Using Contrast-Motion Estimation for the Assessment of the Intra-Aneurysmal Flow Changes Induced by Flow-Diverter Stents. AJNR Am. J. Neuroradiol. 34, 808–815 (2013)
7. Mendes Pereira, V., Ouared, R., Brina, O., Bonnefous, O., Stawiaski, J., Aerts, H., Ruijters, D., van Nijnatten, F., Perren, F., Bijlenga, P., Schaller, K., Lovblad, K.-O.: Quantification of Internal Carotid Artery Flow with Digital Subtraction Angiography: Validation of an Optical Flow Approach with Doppler Ultrasound. AJNR Am. J. Neuroradiol. 35, 156–163 (2014)
8. Brina, O., Ouared, R., Bonnefous, O., van Nijnatten, F., Bouillot, P., Bijlenga, P., Schaller, K., Lovblad, K.-O., Grünhagen, T., Ruijters, D., Mendes Pereira, V.: Intra-Aneurysmal Flow Patterns: Illustrative Comparison among Digital Subtraction Angiography, Optical Flow, and Computational Fluid Dynamics. AJNR Am. J. Neuroradiol. 35, 2348–2353 (2014)
9. Morales, H.G., Bonnefous, O.: Peak systolic or maximum intra-aneurysmal hemodynamic condition? Implications on normalized flow variables. J. Biomech. 47, 2362–2370 (2014)
10. Bonnefous, O., Mendes Pereira, V., Ouared, R., Brina, O., Aerts, H., Hermans, R., van Nijnatten, F., Stawiaski, J., Ruijters, D.: Quantification of arterial flow using digital subtraction angiography. Med. Phys. 39, 6264–6275 (2012)